Application of Tools and Techniques for Carbon Minus Building Construction

Lead Guest Editor: Rahul V. Ralegaonkar
Guest Editors: Deepak Sharma, Hindavi Gavali, and Hemant Chore

Application of Tools and Techniques for Carbon Minus Building Construction

Application of Tools and Techniques for Carbon Minus Building Construction

Lead Guest Editor: Rahul V. Ralegaonkar
Guest Editors: Deepak Sharma, Hindavi Gavali, and
Hemant Chore

Zhaofei Chu, China
Wonseok Chung, Republic of Korea
Donato Ciampa, Italy
Gian Paolo Cimellaro, Italy
Francesco Colangelo, Italy
Romulus Costache, Romania
Liviu-Adrian Cotfas, Romania
Antonio Maria D'Altri, Italy
Bruno Dal Lago, Italy
Amos Darko, Hong Kong
Arka Jyoti Das, India
Dario De Domenico, Italy
Gianmarco De Felice, Italy
Stefano De Miranda, Italy
Maria T. De Risi, Italy
Tayfun Dede, Turkey
Sadik O. Degertekin, Turkey
Camelia Delcea, Romania
Cristoforo Demartino, China
Giuseppe Di Filippo, Italy
Luigi Di Sarno, Italy
Fabio Di Trapani, Italy
Aboelkasim Diab, Egypt
Thi My Dung Do, Vietnam
Giulio Dondi, Italy
Jiangfeng Dong, China
Chao Dou, China
Mario D'Aniello, Italy
Jingtao Du, China
Ahmed Elghazouli, United Kingdom
Francesco Fabbrocino, Italy
Flora Faleschini, Italy
Dingqiang Fan, Hong Kong
Xueping Fan, China
Qian Fang, China
Salar Farahmand-Tabar, Iran
Ilenia Farina, Italy
Roberto Fedele, Italy
Guang-Liang Feng, China
Luigi Fenu, Italy
Tiago Ferreira, Portugal
Marco Filippo Ferrotto, Italy
Antonio Formisano, Italy
Guoyang Fu, Australia
Stefano Galassi, Italy

Junfeng Gao, China
Meng Gao, China
Giovanni Garcea, Italy
Enrique García-Macías, Spain
Emilio García-Taengua, United Kingdom
DongDong Ge, USA
Khaled Ghaedi, Malaysia
Khaled Ghaedi, Malaysia
Gian Felice Giaccu, Italy
Agathoklis Giaralis, United Kingdom
Ravindran Gobinath, India
Rodrigo Gonçalves, Portugal
Peilin Gong, China
Belén González-Fonteboa, Spain
Salvatore Grasso, Italy
Fan Gu, USA
Erhan Güneyisi, Turkey
Esra Mete Güneyisi, Turkey
Pingye Guo, China
Ankit Gupta, India
Federico Gusella, Italy
Kemal Hacıefendioğlu, Turkey
Jianyong Han, China
Song Han, China
Asad Hanif, Macau
Hadi Hasanzadehshooiili, Canada
Mostafa Fahmi Hassanein, Egypt
Amir Ahmad Hedayat, Iran
Khandaker Hossain, Canada
Zahid Hossain, USA
Chao Hou, China
Biao Hu, China
Jiang Hu, China
Xiaodong Hu, China
Lei Huang, China
Cun Hui, China
Bon-Gang Hwang, Singapore
Jijo James, India
Abbas Fadhil Jasim, Iraq
Ahad Javanmardi, China
Krishnan Prabhakan Jaya, India
Dong-Sheng Jeng, Australia
Han-Yong Jeon, Republic of Korea
Pengjiao Jia, China
Shaohua Jiang, China

Chayut Ngamkhanong, Thailand
Trung Ngo, Australia
Tengfei Nian, China
Mehdi Nikoo, Canada
Youjun Ning, China
Olugbenga Timo Oladinrin, United Kingdom
Oladimeji Benedict Olalusi, South Africa
Timothy O. Olawumi, Hong Kong
Alejandro Orfila, Spain
Maurizio Orlando, Italy
Siti Aminah Osman, Malaysia
Walid Oueslati, Tunisia
SUVASH PAUL, Bangladesh
John-Paris Pantouvakis, Greece
Fabrizio Paolacci, Italy
Giuseppina Pappalardo, Italy
Fulvio Parisi, Italy
Dimitrios G. Pavlou, Norway
Daniele Pellegrini, Italy
Gatheeshgar Perampalam, United Kingdom
Daniele Perrone, Italy
Giuseppe Piccardo, Italy
Vagelis Plevris, Qatar
Andrea Pranno, Italy
Adolfo Preciado, Mexico
Chongchong Qi, China
Yu Qian, USA
Ying Qin, China
Giuseppe Quaranta, Italy
Krishanu ROY, New Zealand
Vlastimir Radonjanin, Serbia
Carlo Rainieri, Italy
Rahul V. Ralegaonkar, India
Raizal Saifulnaz Muhammad Rashid, Malaysia
Alessandro Rasulo, Italy
Chonghong Ren, China
Qing-Xin Ren, China
Dimitris Rizos, USA
Geoffrey W. Rodgers, New Zealand
Pier Paolo Rossi, Italy
Nicola Ruggieri, Italy
JUNLONG SHANG, Singapore

Nikhil Saboo, India
Anna Saetta, Italy
Juan Sagaseta, United Kingdom
Timo Saksala, Finland
Mostafa Salari, Canada
Ginevra Salerno, Italy
Evangelos J. Sapountzakis, Greece
Vassilis Sarhosis, United Kingdom
Navaratnarajah Sathiparan, Sri Lanka
Fabrizio Scozzese, Italy
Halil Sezen, USA
Payam Shafigh, Malaysia
M. Shahria Alam, Canada
Yi Shan, China
Hussein Sharaf, Iraq
Mostafa Sharifzadeh, Australia
Sanjay Kumar Shukla, Australia
Amir Si Larbi, France
Okan Sirin, Qatar
Piotr Smarzewski, Poland
Francesca Sollecito, Italy
Rui Song, China
Tian-Yi Song, Australia
Flavio Stochino, Italy
Mayank Sukhija, USA
Piti Sukontasukkul, Thailand
Jianping Sun, Singapore
Xiao Sun, China
T. Tafsirojjaman, Australia
Fujiao Tang, China
Patrick W.C. Tang, Australia
Zhi Cheng Tang, China
Weerachart Tangchirapat, Thailand
Xiaxin Tao, China
Piergiorgio Tataranni, Italy
Elisabete Teixeira, Portugal
Jorge Iván Tobón, Colombia
Jing-Zhong Tong, China
Francesco Trentadue, Italy
Antonello Troncone, Italy
Majbah Uddin, USA
Tariq Umar, United Kingdom
Muahmmad Usman, United Kingdom
Muhammad Usman, Pakistan
Mucteba Uysal, Turkey

Ilaria Venanzi, Italy
Castorina S. Vieira, Portugal
Valeria Vignali, Italy
Claudia Vitone, Italy
Liwei WEN, China
Chunfeng Wan, China
Hua-Ping Wan, China
Roman Wan-Wendner, Austria
Chaohui Wang, China
Hao Wang, USA
Shiming Wang, China
Wayne Yu Wang, United Kingdom
Wen-Da Wang, China
Xing Wang, China
Xiuling Wang, China
Zhenjun Wang, China
Xin-Jiang Wei, China
Tao Wen, China
Weiping Wen, China
Lei Weng, China
Chao Wu, United Kingdom
Jiangyu Wu, China
Wangjie Wu, China
Wenbing Wu, China
Zhixing Xiao, China
Gang Xu, China
Jian Xu, China
Panpan, China
Rongchao Xu, China
HE YONGLIANG, China
Michael Yam, Hong Kong
Hailu Yang, China
Xu-Xu Yang, China
Hui Yao, China
Xinyu Ye, China
Zhoujing Ye , China
Gürol Yildirim, Turkey
Dawei Yin, China
Doo-Yeol Yoo, Republic of Korea
Zhanping You, USA
Afshar A. Yousefi, Iran
Xinbao Yu, USA
Dongdong Yuan, China
Geun Y. Yun, Republic of Korea

Hyun-Do Yun, Republic of Korea
Cemal YİĞİT, Turkey
Paolo Zampieri, Italy
Giulio Zani, Italy
Mariano Angelo Zanini, Italy
Zhixiong Zeng, Hong Kong
Mustafa Zeybek, Turkey
Henglong Zhang, China
Jiupeng Zhang, China
Tingting Zhang, China
Zengping Zhang, China
Zetian Zhang, China
Zhigang Zhang, China
Zhipeng Zhao, Japan
Jun Zhao, China
Annan Zhou, Australia
Jia-wen Zhou, China
Hai-Tao Zhu, China
Peng Zhu, China
QuanJie Zhu, China
Wenjun Zhu, China
Marco Zucca, Italy
Haoran Zuo, Australia
Junqing Zuo, China
Robert Černý, Czech Republic
Süleyman İpek, Turkey

Contents

Research Article

Nanoprocessing of Industrial Rejects for Controlling Operational Energy of Buildings

Sandeep Tembhurkar [iD],[1] **Priyanka Nayar,**[2] **Naumanuddin Azad,**[2] **Rahul Ralegaonkar** [iD],[1] **and Mangesh Madurwar** [iD][1]

[1]*Department of Civil Engineering, Visvesvaraya National Institute of Technology (VNIT), Nagpur, Maharashtra, India*
[2]*Jawaharlal Nehru Aluminium Research Development and Design Centre (JNARDDC), Nagpur, Maharashtra, India*

Correspondence should be addressed to Mangesh Madurwar; mvmadurwar@civ.vnit.ac.in

This study investigates the pozzolanic potential of industrial waste, which fails to meet the chemical composition as defined by the various international standards, e.g., IS: 3812 (Part 1): 2017 and ASTM C618-19 to adopt as a supplementary cementitious material. The effects of mechanical nanoprocessing on pozzolanic reaction efficiency, impact on energy efficiency, and construction affordability were studied. The result of mechanical milling shows the improvement in pozzolanicity, and the physicomechanical characteristics of novel concrete incorporated with identified industrial waste are comparable with control concrete. The building energy simulation was carried out using the BIM software for the house, modelled with controlled concrete, and novel concrete incorporating the identified milled industrial waste. The peak cooling load and building material cost of a novel concrete model house were 34% and 9.09% less than the conventional concrete. The study reveals that the chemical characterization provided in international standards shall not be the only criteria to decide the suitability of the materials to use as supplementary cementitious material, whereas the same can be examined and improved through various treatments, and mechanical nanoprocessing may be one of the best options. Cement production and utilization affect the environment. To reduce the concern, pozzolanic investigation of industrial waste is necessary, which can address the issue of uncontrolled extraction of natural resources, emission, disposal, and pollution globally.

1. Introduction

Industrialization in developing countries has resulted in the consequent accumulation of unmanageable industrial wastes and greenhouse gases (GHGs). Asia produces 4.4 billion tons of solid waste every year [1]. As per the United Nations Environment Programme (UNEP) report, 86 billion tons of carbon dioxide are emitted by global buildings annually [2]. Presently, India alone generates about 290 million tons (MT) of inorganic wastes [3] and 76.4 MT of CO_2 [4] per year from various cement manufacturing industries. Normally, 0.9 ton and 0.1 ton of CO_2 are released into the environment during the manufacturing of 1 ton of cement and 1 ton of concrete, respectively [5, 6]. Cement production (~550 MT by 2020-21) [7]and consumption in

India have increased multifold in the last few decades [8]. The exponential production and consumption of cement and cement products creating a huge environmental burden with the exploitation of natural resources are becoming a global issue [9]. The application of limestone during the clinkering process results in a significant amount of emissions (5-6% of total greenhouse gas emissions) [10–12] by consuming a huge amount of nonrenewable resources [7, 13]. Around 350 to 540 kg of raw slag is generated, from the per ton production of liquid iron and steel [14, 15], and around 24 MT of slag is generated every year in India [16]. The state-wise annual production of steel and iron slag in India is shown in Figure 1.

In the twenty-first century, nanotechnology was a highly adopted technology for research and development in

Steel and Iron Slag (GBFS) produced in India in MTPA

- ■ Chhattisgarh   ■ Karnataka
- ■ Jharkhand   ■ AndharPradesh
- ■ Odisha   ■ Maharashtra
- ■ West Bengal
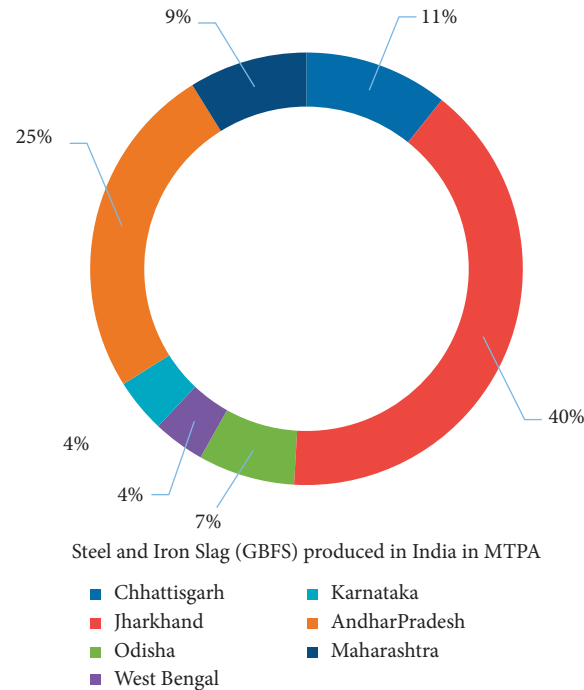
Figure 1: Production of GBFS in FY 2018-19 of India [17, 18].

Table 1: Model details used in the study performance analysis.

Reference	Model	Size of unit in "m"	Areas in Sqm	Wall thickness in "m"	The material used for the study	Code of reference
S.P. Raut et al. [26]	Single room	1×1	1	0.11	Papermill waste (PMW)	
M.V. Madurwar et al. [27]	Single room	1×1	1	0.13	Sugar cane bagasse ash (SCBA)	
R. Chippagiri et al. [21]	Single room	3×3	9	0.1	Co-fired blended ash (CBA)	SP-7-2016 (National Building Code—NBC)
R. Ralegaonkar et al. [28, 29]	1 BHK –GF	Typical	27	0.15 Ext. 0.10 Int.	Bio-fuel ash (BFA)	
H. Gavali et al. [30, 31]	1BHK –GF	Typical	27.5	0.15 Ext. 0.11 Int.	Co-fired blended ash (CBA)	

Note. GF—ground floor, Ext—external wall, Int—internal wall.

construction worldwide [19]. The nanoparticles/nanocomposites have attracted considerable attention as structural materials, because of their low density, high specific modulus, strength, and resistance to wear and corrosion [20]. However, the application of nanotechnology in the development of alternate construction materials needs to be studied in detail. Similarly, energy analysis and cost-effectiveness are also required to be studied for the building energy simulation of alternate nanomaterials [21]. Building information modelling (BIM) is an effective simulation tool that can undertake these parameters [22]. BIM enables the user to create a virtual model to simulate the planning, design, construction, and operational facility in the building [23]. BIM results are object-oriented, intelligent, and provide the digital data of building facilities, generating information on thermal and functional performance, which help to improve the decision and process of establishing the facilities [24, 25]. BIM regulates the life

cycle cost, design, construction, and operational cost of a project [15–17].

Many researchers investigated the thermal performance and embodied energy of building components using the BIM software tool (Revit 2019). The thermal performance of various construction materials developed incorporating industrial wastes was investigated by various researchers using Revit 2019 and is tabulated in Table 1.

Now, there is a need of an hour to find sustainable alternatives to primary binding material (cement) from the enormous available industrial rejects. However, such studies have limitations on the obtained oxide compositions, the particle size of waste material, and their suitability as SCM in accordance with BIS 3812 (Part 1): 2017 [32]. The pozzolanic material not only helps to decrease the burden on natural resources but also encourages to decrease the carbon emission of cement and concrete production. The pozzolanic efficiency of unsuitable industrial waste (as per IS 3812 (Part 1): 2017)

Adopted Methodology
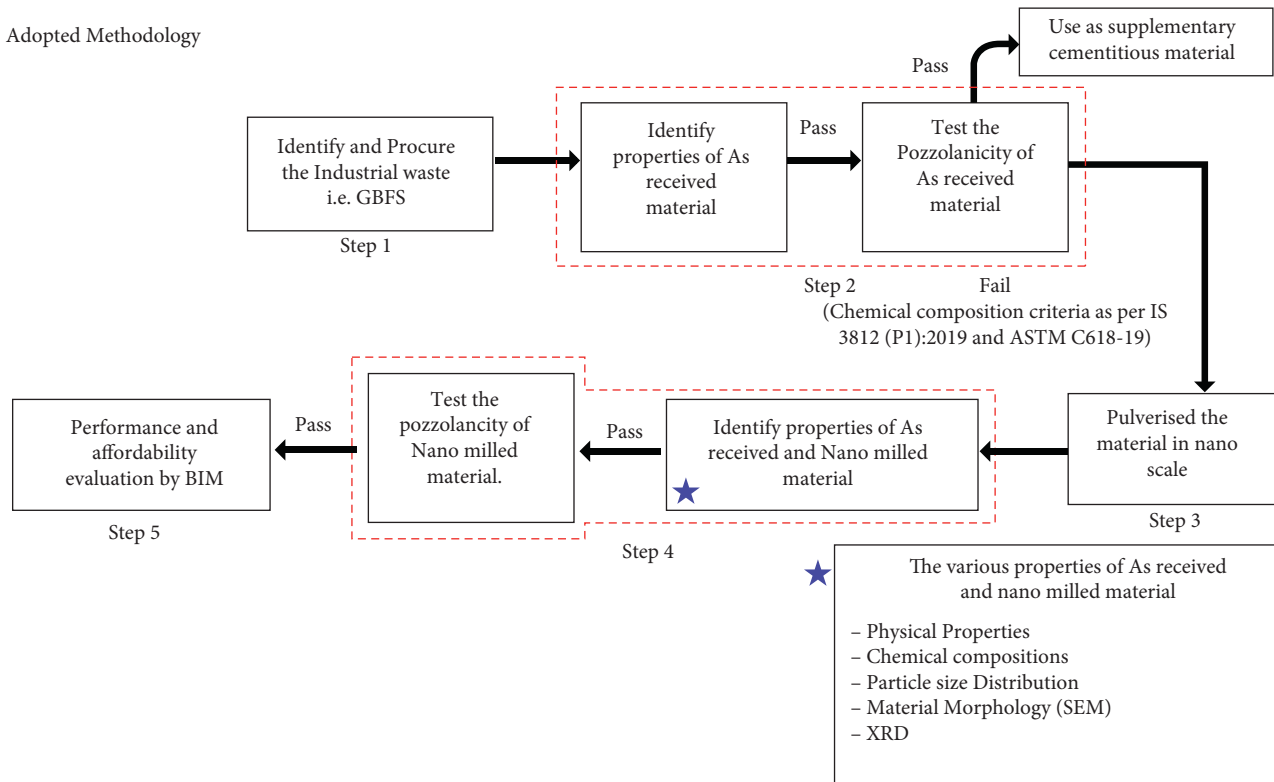
FIGURE 2: Flow diagram for the methodology adopted for the experimental work.

(a)   (b)

FIGURE 3: Identified industrial waste GBFS before and after milling: (a) as-received GBFS and (b) milled GBFS.

was examined after nanoprocessing, i.e., mechanical milling from high-energy ball mill. Introducing the nanotechnology for material milling was found to be an effective treatment to make industrial waste suitable to use as a SCM. In addition to that, the energy efficiency and cost of effectiveness of prototype model were analysed using BIM tool.

2. Materials and Methods

The investigation process is depicted in Figure 2, which explains the step-by-step methodology used in this study. An industrial waste was identified, which was easily available in

and around the study area. Further, the properties of raw materials were identified using the physicochemical and physicomechanical tests and the suitability was checked to use a SCM/pozzolana. If the material fails to meet the criteria to use as a pozzolana, then it must be suitably treated with the best economical option. In this study, mechanical milling treatment was adopted where the material was ground to nanoscale. Subsequently, the properties of milled samples were again tested for pozzolanic efficiency. The treated material with improved pozzolanic efficiency was used for the product development, and later, the performance and affordability of building developed with various building

applications incorporating the treated milled material were analysed using BIM tool.

2.1. Materials Used.

Granulated blast furnace slag (GBFS), an industrial waste, was considered as the principal raw material for the study, which was collected from the iron and steel industry available in and around the research area (Nagpur, Maharashtra, India). OPC 53 grade cement conforming to IS: 12269-2013 [33] was used as a primary binder for laboratory trials. Locally available river sand and crushed stone conforming to IS: 383–2002 [34] were used as fine and coarse aggregates. To perform pozzolanicity tests, necessary chemicals such as saturated calcium hydroxide ($Ca(OH)_2$) solution, calcium oxide (CaO), distilled water, phenolphthalein indicator, the concentrated and 0.1 N hydrochloric acids (HCl), concentrated nitric acid (HNO_3), concentrated sulfuric acid (H_2SO_4), hydrofluoric acid (HF), and Whatman filter paper no. 40 were used.

2.2. Methodology Adopted.

To pulverize the principal raw material to the nanoscale, a high-energy planetary ball mill (Fritsch Pulverisette P5) was used. Milling was optimized using differential time duration of 10, 30, and 90 minutes, i.e., GBFS 10, GBFS 30, and GBFS 90. Figure 3 represents the proposed raw materials, i.e., GBFS, before and after milling. The physical characterization of the material was carried out as per IS 1727-2004 [35]. The physical properties such as specific gravity, bulk density, and setting time of GBFS were tested as per the relevant Indian standards. The nano-structure analysis of identified material was evaluated by particle size distribution (PSD) [36, 37], scanning electron microscopy (SEM) [38, 39], X-ray diffraction (XRD) [40, 41], and X-ray fluorescence (XRF). Grading of mechanically treated ultrafine ground fraction raw materials (granulometric analysis) was performed using a laser particle size analyser [42]. The liquid media was used to conduct the analysis [43]. The ultrasonic frequency was 80 Hz, and the pump speed was 600 rpm. After 10–12 minutes, particle size was assessed. Surface morphology and particle size resemblance of the samples were inspected using the Scanning Electron Micro-Probe Analyzer-JEOL, JAPAN JXA-840. The chemical oxide compositions and loss of ignition (LOI) were evaluated using PANalytical "PW2403 MagiX" XRF technique. Xpert-PRO X-ray diffractometer system was used to analyse the mineral phases of raw and milled material.

Pozzolanicity of principal raw material before and after milling was carried out using various pozzolanicity methods: (i) pozzolanic activity index [44–47], (ii) electrical conductivity [48–50], and (iii) Chapelle activity [44, 51–54]. Pozzolanic activity index (PAI) was evaluated as per the procedure provided in IS 2250:1981. The sample blocks were prepared by replacing 35% (by volume) of OPC with the selected industrial rejects, i.e., GBFS. Pozzolana activity index was calculated in percentage ratio of 28 days of compressive strength of GBFS to the compressive strength of control mortar block [45, 46, 55].

$$\text{Pozzolanic Activity Index (PAI)} = \frac{\text{Compressive Strength of Composition block}}{\text{Compressive Strength of Control block}}. \tag{1}$$

An electrical conductivity test is conducted to study the pozzolanicity of supplementary cementitious materials (SCMs). The sample was prepared using the identified material and calcium hydroxide solution. The water and sample solution was used to find the conductivity of ions present in the material [55, 56]. The Chapelle activity test was performed to determine the fixed CaOH by taking the solution of grounded material in water with CaO and titrating the same with HCL and using phenolphthalein solution as an indicator [54, 55, 57].

$$\text{CA} = 2\frac{[(V_1 - V_2) \times 74 \times 1000]}{V_1 \times 56}, \tag{2}$$

where V_1 is the volume of HCL consumed for titrating solution without pozzolana. V_2 is the volume of HCL consumed for titrating solution containing pozzolana. The suitable building application was developed as an end product using milled GBFS samples and compared over the conventional building application of the same grade for energy efficiency using the BIM simulation tool.

3. Model Development

After the micro-analysis of identified material, the pozzolanic performance of mechanically milled material was evaluated to check the sustainability of materials and treatment process. On suitability of materials, a novel construction concrete building application was cast incorporating the mechanically milled (treated) industrial waste, and later, a model house was simulated in BIM software for conventional and novel concrete elements to study the energy efficiency and affordability.

BIM tool is used for 3D design and modelling, which helps in forecasting the building design, assembly of elements, and work progress [40, 41]. A single-storey residential building was selected for BIM model. The project was situated in Indore, Madhya Pradesh, under the lightweight housing scheme of Global Housing Technology Challenge (GHTC), Government of India. The project aims to provide a sustainable technology solution for faster and cost-effective construction suitable for the geo-climatic zones and hazardous conditions.

Figure 4 shows the 2D plan of building, and Autodesk AutoCAD 2019 version was used to draw the plan. The plan of a single dwelling unit has an area of 29.92 m². The carpet area was also approved by the GHTC, India [58]. The prototype model of the same project was analysed for the study area, Nagpur, Maharashtra, India (latitude 21.1311°N and longitude 79.0511°E). The residential building mainly consists of three rooms, i.e., living room, a bedroom, and a kitchen with a small passage and toilet. Clear 3 m height of the unit was considered. The thickness of the exterior and internal walls was considered 150 mm and 100 mm, respectively. Three windows, W1, W2, and W3 of sizes 1.5 m × 1.2 m, 1 m × 1.2 m, and 0.8 m × 1.2 m, respectively, were provided. The doors D1, D2, D3, and D3A of size 1.2 m × 2.1 m, 1 m × 2.1 m, 0.75 m × 2.1 m, and 0.9 m × 2.1 m, respectively, were provided in the building. For the base case, the model developed with elements of conventional concrete was considered, whereas the alternate model developed with building application of the same grade incorporating milled GBFS was considered for comparative analysis. The peak cooling load demand was calculated for both the models. The temperature range of 18–28°C for the climate zone of Nagpur (21.1311°N-79.0511°E) was set as per the SP 41 (BIS-1987) [59]. Each room of the building was analysed for the design cooling load using the building information modelling tool (BIM) that is the Revit Architecture 2019 Student Version [60]. Two separate models were simulated for analysis where the walls, floor, and slab of the building were considered with the properties of respective materials.

4. Results and Discussion

The results of the tests performed on as-received and mechanical-processed industrial waste are discussed as follows.

4.1. Physical Properties.

The results of the physical characterization are shown in Table 2. From the test results, it was observed that the specific gravity of industrial waste before and after milling remains unchanged and was found lower than the specific gravity of cement; hence, it was expected that the building material incorporating these wastes will be lighter in weight. The density of material was determined before and after milling; there was no discernible difference observed in the density of GBFS after milling. The initial setting time of the proposed industrial waste was higher than the cement, whereas the final setting time is lower than the cement, which is further diminished significantly on milling. The surface area of industrial waste increases exponentially on milling. The negligible evidence of soundness and shrinkage percentage was noticed before and after milling; hence, it can be recommended for suitable building applications. Milled GBFS showed considerable improvement in lime reactivity.

In Table 3, characteristics of before (0 min) and after milled (90 min) GBFS are displayed according to the criteria mentioned in Table 2 of BIS 3812 (Part 1): 2017. The comparative study was carried out on basis of fineness: wet sieving, lime reactivity strength, 28 days of compressive strength, and soundness of material. 126% improvement in fineness was noticed after milling the sample than that of the before milled sample and meeting the requirement of BIS. Particles retained on 45 micron IS sieve using the wet sieving method before and after milling show the result of 24% and 100%, respectively, whereas the minimum requirement is 34%. The improvement in fineness must be the result of the mechanical nanoprocessing. The lime reactivity of milled samples improves significantly after mechanical milling and achieved 85% more strength than the BIS, i.e., IS 3812 (Part 1): 2017. The compressive strength of milled samples was increased by more than 100%. The observed improvement is due to the particle packing and well compaction of nano-particles. Negligible soundness was observed before and after milling, which shows the suitability to mix the material in principle binding material cement for various building applications/products.

4.2. X-Ray Fluorescence (XRF).

Table 4 shows the chemical composition of the proposed industrial waste. It was observed that the milling treatment had no discernible influence on the chemical compositions and LOI values of the materials.

The amorphous (% reactive) silica plays a major role in the pozzolanic activity of the materials as per the provisions prescribed by BIS 3812 (Part 1): 2017. From the obtained results of XRF, it was observed that the industrial waste, i.e., GBFS, fails to meet the criteria mentioned in Table 1, BIS 3812 (Part 1): 2017, and hence, it is not suitable for the use as supplementary cementitious material even though the LOI is within the acceptable range as prescribed by the same BIS. The criteria given in BIS for the combined percentage of Al, Si, and Fe were also not satisfied by the GBFS milled sample.

4.3. X-Ray Diffraction (XRD).

Figure 5 shows X-ray diffraction analysis of as-received and milled samples of GBFS. The graph was plotted diffraction angle (2θ) versus intensity count, where the diffraction angle was stated from 10-degree angle and raised up to 70° on x-axis. The intensity of peaks for as-received sample and optimized milled sample (90 min grinding duration) was started from 140 counts and 150 counts, respectively, and this shows that the GBFS absorbed the energy on milling. Graphs A and B show the XRD phase of as-received and milled GBFS. The flattered hump between 20° and 35° diffraction angle and intensity depicts the amorphous phase of an as-received and milled sample of GBFS. There is no significant change observed in the XRD phase before and after milling of GBFS. Hence, as-received and milled GBFS was expected to participate in hydration reaction due to the presence of amorphous silica.

4.4. Scanning Electron Microscopy (SEM).

Figure 6 shows the surface morphology and particle size resemblance measured by scanning electron microscopy (SEM). The image shows the particle agglomeration after the high-energy milling
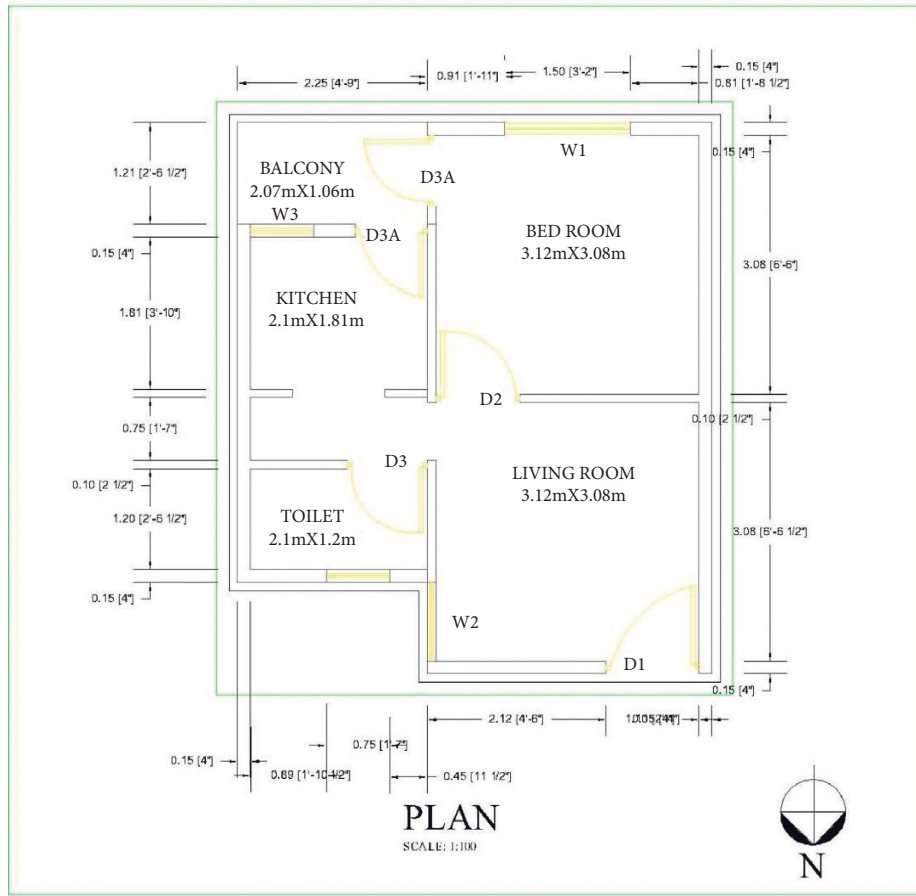
FIGURE 4: AutoCAD 2D plan for single dwelling unit.

TABLE 2: Physical characterization of GBFS.

Characterization	Cement	GBFS		Remarks
		As-received	Milled	
Specific gravity	3.15	2.84	2.83	—
Density (kg/m^3)	1430	1500	1490	—
Initial setting (min)	30	40	35	—
Final setting (min)	600	430	355	—
pH	8.00	8.90	9.15	—
Soundness (%)	4.50	−0.0016	−0.01	Negligible
Dry shrinkage (%)	—	−0.043	−0.062	Negligible

process, even after individual particle size reached the nanoscale range. The particle size increased due to the agglomeration was highlighted in yellow circle, which shows the deposition of more than one particle. This agglomeration temporary occurs because of the van der Waals force of attraction, in which particle is obtained after high-energy milling. Therefore, the values after final milling, i.e., 30 min and 90 min of material, show the enlargement in size of particles. GBFS was milled for 90 minutes and resulted in particles of sizes ranging from 50 to 600 nm, respectively.

4.5. Laser Particle Size Analysis.

Figure 7 represents the laser particle size distribution of proposed industrial rejects. The size of particle scales on D_{10} (10% particles passing), D_{50} (average passing), and D_{90} (90% particles passing) is depicted in Table 5, respectively. The as-received sample was milled for 10, 30, and 90 minutes in a high-energy planetary mill to bring it to nanolevel. Insignificant variation in the particle size was observed after milling for 10 to 30 min of duration. The average particle size of as-received sample was observed to be 331 nm on 10 min of milling and the sample size was observed to be 344 nm, whereas on 30 min of milling the sample size was observed to be 328 nm; this may be due to the surface charge increments in particles. After that, a large reduction in the particle size was observed for a milling duration of 90 min. The D_{50} of agglomerated GBFS (i.e., GBFS-WM) shifted to 384 nm from 331 nm on 90 min of milling. It was observed that the enlarged surface area after milling is due to van der Waals force of attraction or surface charge, in which particles acquire after milling. Therefore, the values of the final grinding, i.e., 90 min of GBFS, show the increment in size of particle, which is reflected in Table 5.

4.6. Pozzolanic Activity Tests.

From the proposed industrial waste, the results obtained for GBFS are contradictory. As per the requirement of BIS 3812 (Part 1): 2017, the material may not be suitable to be used as SCM, whereas the XRD pattern and lime reactivity of the sample emphasize the

TABLE 3: Physical characterization of GBFS with respect to IS 3812(P1)-2013.

Sr. No.	Characteristics	GBFS		Requirements as IS 3812(P1)-2017
		BM 0 min	AM 90 min	
1	Fineness—specific surface in m^2/kg by Blaine's permeability method, min	153<	347>	320
2	Particles retained on 45 micron IS sieve (wet sieving) in percent 1), max	23<	0<	34
3	Lime reactivity—average compressive strength in N/mm^2, min	3.83<	8.31>	4.5
4	Compressive strength at 28 days in N/mm^2, min	76<	100>	Not less than 80 percent of the strength of corresponding plain cement mortar cubes
5	Soundness by autoclave test—expansion of specimen in percent, max	−0.0016<	−0.01<	0.8

Requirement as per Table 2 of IS 3812: 2017 Clause Nos. 5.1 and 7.1.

TABLE 4: XRF analysis of before and after milled samples.

Sample ID/composition	GBFS -WM	GBFS-10	GBFS-30	GBFS-90	OPC cement	IS 3812: 2013
Na$_2$O	0.38	0.2	0.2	0.2	—	1.5 max
MgO	7.61	8.0	8.45	8.5	3.4	5 max
Al$_2$O$_3$	12.24	12.76	13.69	14.67	5.5	—
SiO$_2$	31.76	31.63	31.71	32.11	25.1	35 min
P$_2$O$_5$	0.01	0.01	0.01	0.01	—	—
SO$_3$	1.75	1.76	1.73	1.69	2.7	3 max
K$_2$O	0.6	0.61	0.65	0.69	0.5	—
CaO	43.36	42.31	41.85	40.75	55	—
TiO$_2$	0.52	0.53	0.53	0.51	—	—
MnO$_2$	0.29	0.03	0.3	0.32	—	—
Fe$_2$O$_3$	0.46	0.61	0.41	0.40	5.9	—
LOI	0.68	1.26	0.19	0.15	0.9	5 Max
Al + Si + Fe	44.46	45	45.81	46.18	36.5	70 min

(a)
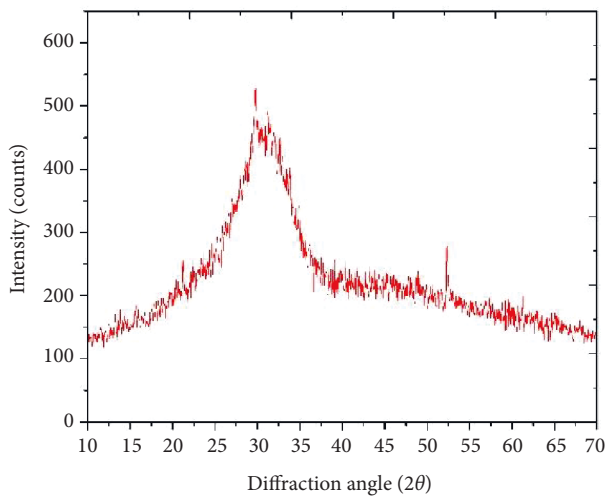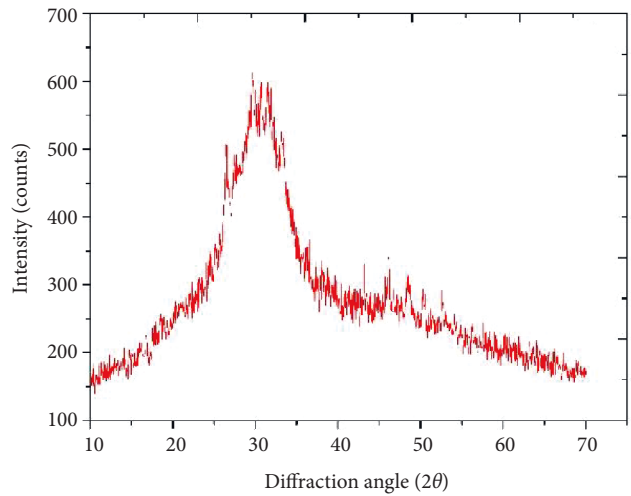
(b)

FIGURE 5: X-ray diffraction of GBFS (a and b).

industrial wastes to be considered as SCM. The pozzolanicity tests were performed before and after milled material to study the effect of mechanical processing on pozzolanic properties.

4.6.1. *Pozzolanic Activity Index (PAI)—Strength Determination.* The observed compressive strength and the trends of compositions established with the effect of milling are shown in Table 6 and regression patterns as shown in
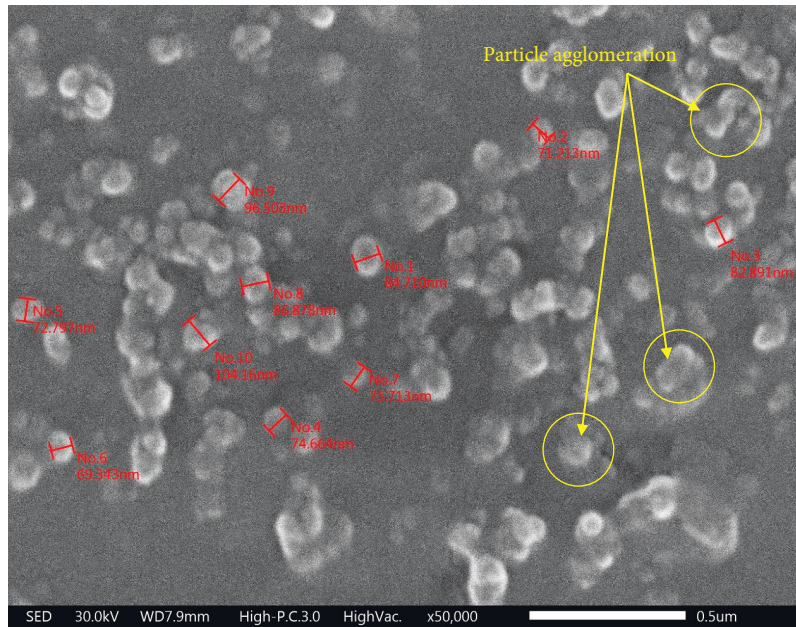
FIGURE 6: SEM micrographs of post-milled raw materials. GBFS 100–600 nm particle size.

TABLE 5: Particle GBFS size.

Sample ID	Time (min)	D10	D50	D90	Surface area of the particles in (m²/kg)
GBFA	0*	248	**331**	453	153
	10	257	**344**	474	186
	30	249	**328**	445	254
	90	288	**384**	526	347

*As-received material is denoted by the zero minutes (0 min).
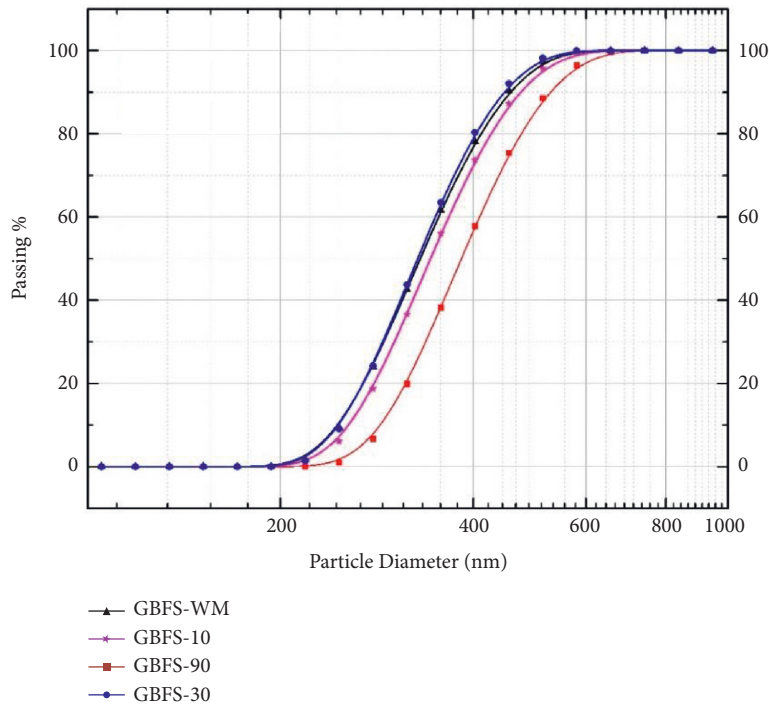
FIGURE 7: Particle size analysis of GBFS.

TABLE 6: Test results of all materials.

| Samples | Milling duration (minute) | PAI (%) | | Electrical conductivity (μS/cm) | | | Chapelle activity (mg Ca(OH)$_2$/g sample) | | |
		%	Remarks	EC drop	EC in %	Remarks	mg Ca(OH)$_2$/g sample	CA in %	Remarks
Control mortar	—	100	—	5.88	—	—	—	—	—
GBFA	WM	76.5	>75% of controlled compressive strength. Hence satisfied	4.63	78.74	>1.2 hence good pozzolanic (pozzolanicity improved on mechanical milling)	245.85	37.25	Pozzolanicity improved on mechanical milling and satisfies the requirement on 90 min of milling
	10	80.37		5.072	86.26		430.23	65.19	
	30	86.6	Pozzolanicity improved on mechanical milling	5.02	85.37		553.16	83.81	
	90	100		5.097	86.68		799	121.06	
Standard	—	ASTM-C311 [61]		>1.2 (Lexan-1989)			>660 (NF P18-513)		

Figure 8. The graph was plotted for milling duration (in minutes) versus pozzolana activity index of GBFS (in %). The significant improvement was observed in PAI results of after milled samples as compared to as-received sample. The trend of the linear line shows the high regression value, i.e., 0.92. It can be explained as an effect of mechanical supplementary fillers; as the fineness increases, the surface area of the matrix also increases, thereby enhancing the formation of intermolecular compounds. Nanoprocessed amorphous silica further leads to the formation of secondary C-S-H compounds. The PAI method was adopted as specified in Brazilian standard NBR 12653:1990 for the pozzolanic material testing. The R^2 values obtained from the regression (Figure 8) show the significant improvement in the pozzolanic rate of reaction in GBFS on milling.

4.6.2. Electrical Conductivity Test (ECT).

To evaluate and ensure the material's pozzolanic reactivity, an electrical conductivity test was also performed. The electrical conductivity of saturated Ca(OH)$_2$ at $40 \pm 1°$ temperature was 7.98 mS/cm noticed. The concentration of calcium and hydroxyl ion reduces with time, which could be noticed from the decrement in conductivity values of GBFS solution. The results reveal the reaction between the silica present in GBFS and the Ca(OH)$_2$ standard solution, which formed the C-S-H gel. The R^2 value obtained from the regression (Figure 9) for GBFS was 0.96, which shows the significant improvement in pozzolanic rate of reaction due to mechanical milling.

4.6.3. Chapelle Activity Test.

Chapelle activity is carried out to evaluate the consumed Ca(OH)$_2$ in the pozzolanic reaction. Pozzolanic material is added to the hydrated cement paste, so that silica reacts with the Ca(OH)$_2$ to produce secondary C-S-H gel [43]. The larger surface area of pozzolanic material increases the rate of pozzolanic reaction, and the amount of reaction produces secondary C-S-H gel.

Figure 10 shows the trend of the Chapelle activity for GBFS. A significant increase in the consumed Ca(OH)$_2$ was observed due to the milling treatment for all the samples. The best results were fitted in the linear mathematical model. The
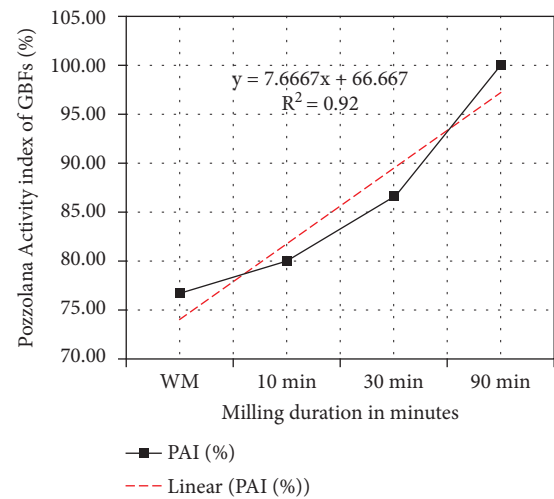
FIGURE 8: Pozzolanic activity index of GBFS.
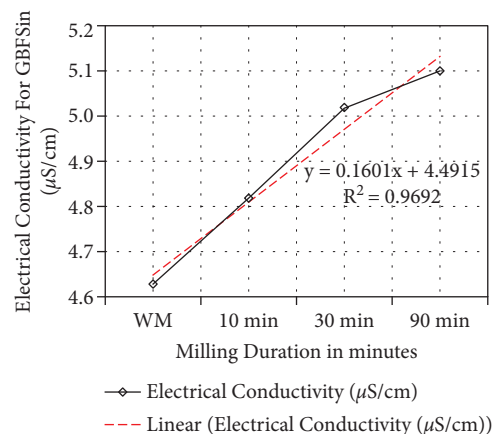
FIGURE 9: Electrical conductivity of GBFS for different grinding times.

R^2 value obtained for GBFS is 0.983. The observed regression model was significant and effective, as the R^2 value was close to 1, whereas, from Table 6, it was observed that the Chapelle activity of GBFS was better than the standard values. Chapelle
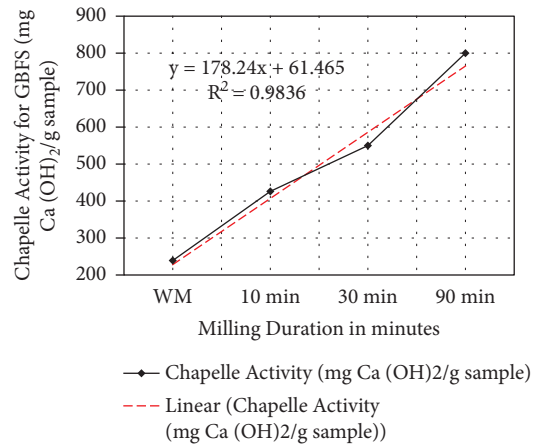
Figure 10: Chapelle activity of GBFS.
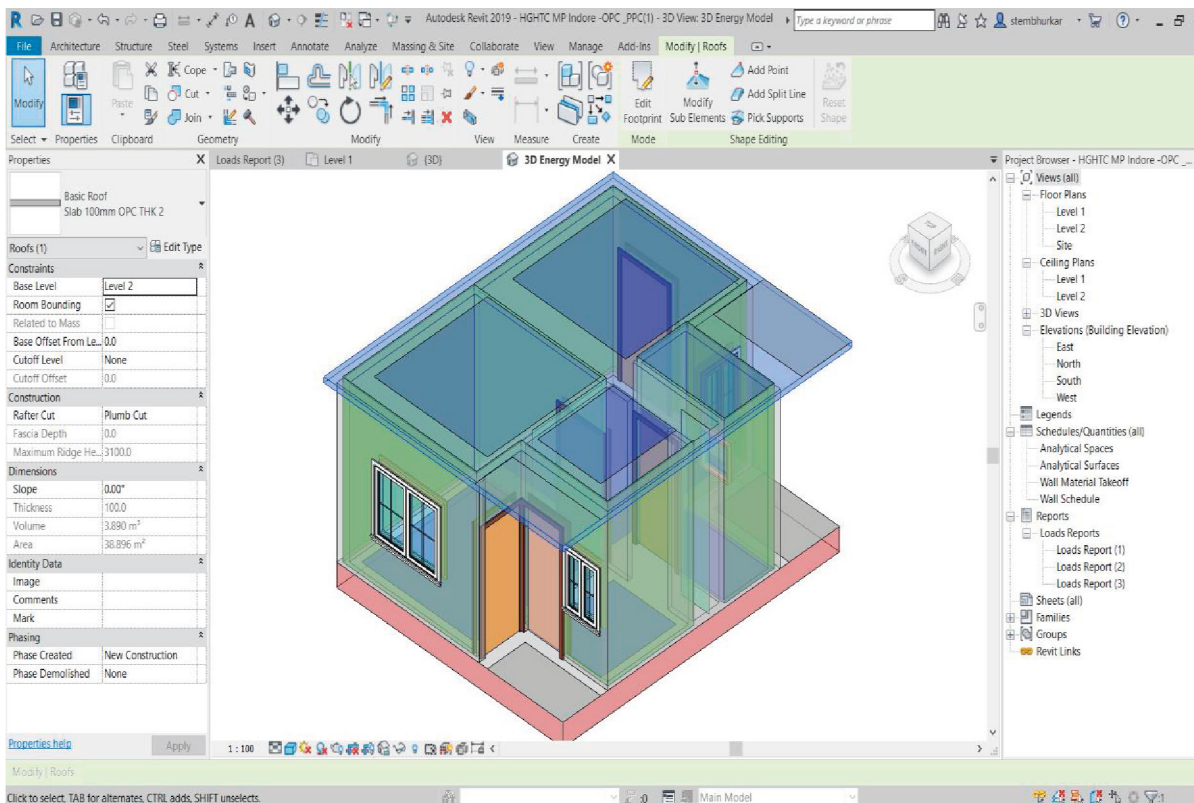
Figure 11: Energy analysis models in Revit.

activity values should be greater than 660 mg Ca(OH)$_2$ per gram of sample as recommended in NF P18-513.

5. Performance and Affordability Evaluation

A comparative study carried out by Azhar et al. [24] for analysis of building performance revealed that the virtual environment is the most powerful and versatile software tool followed by Ecotect and Green Building Studios. Shoubi et al. [60] used Revit Architecture and Ecotech for energy analysis of building having an area of 400 m^2 two-storey unit where the composite material was proposed

for saving operations energy of buildings. Gavali et al. [28, 29, 61] simulated a single-storey load-bearing model in Nagpur, India. The products were developed incorporating the co-fired blended ash (CBA) and fly ash bricks. The analysis was carried out using Revit Architecture BIM tool. The analysis concluded that deploying CBA bricks in construction would potentially lower the cost and energy of the building in comparison with fly ash brick. The above discussion emphasized and justified the use of the BIM tool for assessing the thermal performance, energy analysis, and affordability of buildings [64]. Hence, the Revit Architecture 2019 (Student Version)

TABLE 7: Comparative study of material along with thermal properties.

Material ID	Density kg/m³	Thermal conductivity (W/m-k)	Peak cooling load W	Embodied energy (EE) MJ	Cost/cum (material cost) (₹ in Lac)
GBFS	2475 (<0.8%)	0.92 (<34.3%)	17929 (<34%)	24116 (<26.72%)	2.30 (<9.09%) (US$-3052.30)
OPC concrete	2495(100%)	1.40 (100%)	27089(100%)	32908 (100%)	2.53 (100%) (US$-3357.53)
Reference		IS 9489 (1980)	HVAC report (2011)		Local market rate

simulation tool was used for energy analysis and affordability study.

Models were simulated for a design mix of M30 grade concrete. The base model was considered with conventional concrete using OPC 53, and the alternate model was with replacing the 30% of OPC by milled GBFS industrial waste. The model is shown in Figure 11. The concrete made up of industrial waste was tested for physicomechanical properties after 28 days of wet curing. The physicomechanical properties show the desirable results over the conventional concrete. The density of concrete made from GBFS was noticed as 0.8% lower than control concrete, and this shall be due to the decreased specific gravity of GBFS (10%) when compared with OPC. To evaluate the energy analysis of the models, the thermal conductivity of GBFS concrete was examined as per the IS 9489:2017 [62]. The thermal conductivity of GBFS concrete is observed 34.3% lower than control concrete of the same grade.

For building simulation, the product properties need to be incorporated into the BIM software such as thermal conductivity and density. The simulation resulted in space heating and cooling load inside the dwelling unit, where the peak cooling load was estimated for the individual model. All elements of the dwelling unit were considered with the same material properties for slab, floor, and walls. The peak cooling load of GBFS model was found 34% lower than the base model cast with control concrete. The significant change was noticed in the results of the functional analysis of GBFS over control concrete. Also, a noticeable variation was observed in the affordability analysis. BIM software revealed that the total concrete volume for the single-family unit is 11.42 m³. The cost of concrete ingredients was based on current and prevailing market rates near the research area. The energy cost of mechanical milling was considered in case of concrete applications incorporating industrial waste. The mechanical milling of industrial waste requires an energy of 0.0043 MJ/kg. The cost of transportation, labour, and equipment in both the cases are location-specific and equivalent hence not considered for cost analysis. The BIM models show that the cost of GBFS concrete is 9.09% lower than the cost of control concrete. Table 7 shows the comparative study of material along with thermal properties.

6. Conclusions

The aim of this work was to compare the operational energy of a building developed with novel materials incorporating nanoprocessed industrial waste, which was unsuitable to use as SCM over the conventional material. In the first part of this study, the pozzolanic performance is evaluated of nanoprocessed industrial waste where the appropriate direct and indirect pozzolanicity tests are used. The results obtained from the tests show that the treatment has a potential to make non-SCM to active mineral admixture.

The mechanical milling of GBFS for the optimized duration of 90 minutes, respectively, reduces the particle size of GBFS up to nanolevel, which increases the surface area of the material by 226% with a subsequent increase in the pozzolanic rate of reaction. SEM showed an increase in particle size of identified industrial waste in mechanical milling due to the phenomenon of agglomeration. GBFS meets the requirements of SCM as per the IS 3812: 2013 except for silica percentage. The pozzolanic performance was evaluated from the obtained results of the pozzolanic activity index (PAI), Chapelle activity (CA), and electrical conductivity (EC). The GBFS PAI meets the strength requirements at optimized duration. The results of the Chapelle activity showed that the amount of $Ca(OH)_2$ consumed in milled GBFS is 224.99% as compared to as-received GBFS. The milled GBFS sample showed the better pozzolanic performance by 21% compared with the criteria mentioned in NFP 18-513.

The identified materials (GBFS) showed a significant electrical conductivity drop when tested for pozzolanicity. The electrical conductivity drops for milled GBFS increased by 10% compared with as-received sample. The linear regression models of the pozzolanic activities and milling duration were established. The R^2 values of PAI, CA, and EC test of GBFS have a range of 0.70–0.99 for all pozzolana tests. The ultrafine particles of GBFS significantly improve pozzolanicity. This could lead to the maximum replacement of cement in concrete production. Ultimately, it will reduce greenhouse gas emissions and will help the cement industry to become more sustainable. Furthermore, it will provide the solution to the problem of waste disposal and pollution.

In the second part, BIM tool was used to develop the simulation model and evaluate the energy performance and cost analysis of material. The BIM tool evaluated the operational peak cooling and heating load of material after simulation. The main sources of energy efficiency of building were external walls, windows, and doors, which are foist heating and cooling load on structure. BIM tool offers the opportunity to connect all particulars of building to measure operational energy consumption, cost of building components with treated material, etc. This method can be adopted for any building to calculate the load on elements of structure by selecting the alternative material, which reduced the energy consumption and environmental impact.

The critical analysis result shows the performance study of Industrial rejects GBFS consisting of low thermal conductivity as compared to control concrete. The peak cooling

load of GBFS model was 34% lower than control concrete, reducing the significant energy consumption of the building. Using industrial waste, the cost of construction was reduced by 9% to conventional building cost, and it was observed that the GBFS can give a more effective solution as a sustainable and economical material. This study encourages the utilization of BIM tool to analyse the innovative materials for the energy consumption, life cycle analysis, and time cost analysis for the future studies.

The overall results reveals that the mechanical milling may not improve the chemical characteristics of material, but it can enhance the pozzolanicity and physical properties of wastes. Therefore, such milled industrial wastes can be a promising material for the concrete manufacturing after designing a mix and trials. This material can also be adopted as the alternative of cement, which can reduce the carbon footprints and energy emission and prove the affordable materials for the future construction industry.

Abbreviations

Al: Aluminium
Al_2O_3:   Aluminium oxide
BFA: Bio-fuel ash
BIS: Bureau of Indian Standards
BIM: Building information of modelling
CA: Chapelle activity
$CaOH_2$:   Calcium hydroxide
CBA: Co-fired blended ash
CO_2:   Carbon dioxide
C-S-H: Calcium silicate hydrate
CSR: Schedule rate
EC: Electrical conductivity
EE: Embodied energy
Fe: Iron
FY: Financial year
GBFS: Granulated blast furnace slag
GHG: Greenhouse gases
GHTC: Global housing technology challenge
HF: Hydrofluoric acid
HNO_3:   Nitric acid
H_2SO_4:   Concentrated sulfuric acid
LS: Lime sludge
MgO: Magnesium oxide
MTs: Million tons
OPC: Ordinary Portland cement
PAI: Pozzolanic activity index
PMW: Papermill waste
PWD: Public Works Department
P_2O_5:   Phosphorus pentoxide
SCBA: Sugar cane bagasse ash
SCM: Supplementary cementitious material
SEM: Scanning electron microscopy
SiO_2:   Silicon dioxide
SO_3:   Sulfur trioxide
TiO_2:   Titanium dioxide
UNEP: United Nations Environment Programme
WM: Without milled
XRD: X-ray diffraction
XRF: X-ray fluorescence.

Data Availability

Data statements will be made available whenever required.

Additional Points

(i) Mechanical milling was used for nanoscaling of identified industrial waste. (ii) The pozzolanic properties of industrial waste were improved through nanoscaling. (iii) The building energy simulation was studied using the BIM tool. (iv) Peak cooling load and building cost is 34% and 9.09% lower than conventional ones.

Disclosure

Statement of Novelty. In this research, an industrial waste that fails to meet the pozzolanic criteria, as per the BIS 3812 (Part 1): 2017 and ASTM C618-19, was selected. The pozzolanicity results were validated and statistically established through various available pozzolanicity test methods and microstructure analyses. Also, a holistic approach is adopted by assessing the energy and cost efficiency of modelled building unit developed by incorporating treated industrial waste over the conventional through building information modelling (BIM) tool. This shall lead to a new pathway to utilize the industrial rejects as a partial replacement of the cement in construction industry, which will reduce the carbon emission of cement industry.

Conflicts of Interest

The authors declare that they have no conflicts of interest.

Acknowledgments

References

[1] M. v. Madurwar, R. v. Ralegaonkar, and S. A. Mandavgane, "Application of agro-waste for sustainable construction materials: a review," *Construction and Building Materials*, vol. 38, pp. 872–878, January. 2013.

[2] H. Liu, J. Li, Y. Sun, Y. Wang, and H. Zhao, "Estimation method of carbon emissions in the embodied phase of low

carbon building," *Advances in Civil Engineering*, vol. 2020, Article ID 8853536, 9 pages, 2020.

[3] A. Pappu, M. Saxena, and S. R. Asolekar, "Solid wastes generation in India and their recycling potential in building materials," *Building and Environment*, vol. 42, no. 6, pp. 2311–2320, June. 2007.

[4] I. Tiseo, "Annual change in carbon dioxide (CO2) emissions in India 1982-2020," Statista," 2021, https://www.statista.com/statistics/1119152/annual-carbon-dioxide-change-in-india/.

[5] Ž. Rudžionis, S. K. Adhikary, F. C. Manhanga et al., "Natural zeolite powder in cementitious composites and its application as heavy metal absorbents," *Journal of Building Engineering*, vol. 43, November. 2021.

[6] A. Mehta and D. K. Ashish, "Silica fume and waste glass in cement concrete production: a review," *Journal of Building Engineering*, vol. 29, May 01, 2020.

[7] D. Kumar Ashish and S. Kumar Verma, "Cementing Efficiency of Flash and Rotary-Calcined Metakaolin in Concrete," *Journal of Materials in Civil Engineering*, vol. 31, 2019.

[8] I. Ministry Of commerce & industry, GoI, "cement industry in India," The ASHA Leader," vol. 25, no. 1, pp. 22–24, 2020, https://www.ibef.org/industry/cement-india.aspx#login-box.

[9] S. Goswami, D. K. Shukla, and P. K. Singh, "Sustainable transformation of sewage sludge ash and waste industrial additive into green cement blend," *Structural Concrete*, 2021.

[10] S. K. Adhikary, D. K. Ashish, and Ž. Rudžionis, "Expanded glass as light-weight aggregate in concrete – a review," *Journal of Cleaner Production*, vol. 313, September. 01, 2021.

[11] S. K. Adhikary, Ž. Rudžionis, S. Tučkutė, and D. K. Ashish, "Effects of carbon nanotubes on expanded glass and silica aerogel based lightweight concrete," *Scientific Reports*, vol. 11, no. 1, December. 2021.

[12] S. K. Adhikary, D. K. Ashish, and Ž. Rudžionis, "Aerogel based thermal insulating cementitious composites: a review," *Energy and Buildings*, vol. 245, August. 15, 2021.

[13] K. S. Devi, V. V. Lakshmi, and A. Alakanandana, "Impact of cement industry on environment – an overview," *Asia pacific journal of research*, vol. 1pp. 156–161, Lvii, 2017.

[14] Indian Bureau of Mines, "Indian minerals yearbook 2018 (part- II metals and alloys)," *Ministry of Mines Indian Bureau of Mines*, vol. 2018, no. 0712, pp. 1–9, 2019, https://mitra.ibm.gov.in/Documents/IMYB/Vol.%20II%20Reviews%20on%20Metals%20and%20Alloys/03132018114602Antimony%20AR%202017.pdf.

[15] D. K. Ashish, B. Singh, and S. K. Verma, "The effect of attack of chloride and sulphate on ground granulated blast furnace slag concrete," *Advances in concrete construction*, vol. 4, no. 2, pp. 107–121, June. 2016.

[16] I. Bhavan, *Indian Minerals Yearbook 2018 (Part-III :Minaral Reviews 57 th Edition*, Iron ore (FINAL RELEASE) Government of India Ministry of Mines Indian Bureau of Mines, Nagpur, 2019.

[17] Niti Aayog, "Strategy paper on resource efficiency in steel sector through recycling of scrap & slag," Ministry of Steel, Government of India," 2018, https://niti.gov.in/content/circular-economy-and-resource-efficiency.

[18] B. Thacker, "Indian Paper Sector 06," vol. 91, no. August, pp. 1–134, 2018.

[19] W. Zhu, P. J. M. Bartos, and A. Porro, "Application of nanotechnology in construction Summary of a state-of-the-art report," *Materials and Structures/Materiaux et Constructions*, vol. 37, no. 273, pp. 649–658, 2004.

[20] S. C. Tjong and K. F. Tam, "Mechanical and thermal expansion behavior of hipped aluminum-TiB 2 composites,"

Materials Chemistry and Physics, vol. 97, no. 1, pp. 91–97, 2006.

[21] R. Chippagiri, H. R. Gavali, R. v. Ralegaonkar, M. Riley, A. Shaw, and A. Bras, "Application of sustainable prefabricated wall technology for energy efficient social housing," *Sustainability*, vol. 13, no. 3, pp. 1–12, 2021.

[22] M. Motalebi, A. Rashidi, and M. M. Nasiri, "Optimization and BIM-based lifecycle assessment integration for energy efficiency retrofit of buildings," *Journal of Building Engineering*, vol. 49, May 2022.

[23] S. Azhar, "Building information modeling (bim): trends, benefits, risks, and challenges for the aec industry," *Leadership and Management in Engineering*, vol. 11, no. 3, pp. 241–252, 2011.

[24] S. Azhar, J. Brown, and R. Farooqui, "BIM-based sustainability analysis: an evaluation of building performance analysis software," in *Proceedings of the 45th ASC Annual Conference*, pp. 1–4, Gainesville, Florida, USA, 2009.

[25] S. Azhar, M. Khalfan, and T. Maqsood, "Building information modeling (BIM): now and beyond," *Australasian Journal of Construction Economics and Building*, vol. 12, no. 4, pp. 15–28, 2012.

[26] S. Raut, S. Mandavgane, and R. Ralegaonkar, "Thermal performance assessment of recycled paper mill waste–cement bricks using the small-scale model technique," *Journal of Energy Engineering*, vol. 140, no. 4, Article ID 04014001, 2014.

[27] M. v Madurwar and R. v Ralegaonkar, "Controlling indoor air temperature using bagasse ash bricks," *Proceedings of the Institute of Civil Engineers: Engineering Sustainability*, vol. 168, no. 2008, 2015.

[28] R. v. Ralegaonkar, H. R. Gavali, V. v. Sakhare, A. J. Puppala, and P. B. Aswath, "Energy-efficient slum house using alternative materials," *Proceedings - Institution of Civil Engineers: Energy*, vol. 170, no. 3, pp. 93–102, August. 2017.

[29] R. v. Ralegaonkar, H. R. Gavali, V. v. Sakhare, A. Puppala, and P. B. Aswath, "Application of sustainable construction materials for urban slum houses," *International Journal of Environment and Sustainable Development*, vol. 8, no. 3, pp. 182–186, 2017.

[30] H. R. Gavali, A. Bras, and R. v. Ralegaonkar, "Cleaner construction of social housing infrastructure with load-bearing alkali-activated masonry," *Clean Technologies and Environmental Policy*, vol. 23, Article ID 0123456789, 2021.

[31] H. R. Gavali and R. v. Ralegaonkar, "Application of information modelling for sustainable urban-poor housing in India," *Proceedings - Institution of Civil Engineers: Engineering Sustainability*, vol. 172, no. 2, pp. 68–75, 2018.

[32] B. of Indian Standards, "IS 3812-2 (2033): specification for pulverized fuel ash, Part 2: for use as admixture in cement mortar and concrete," 2013.

[33] B. of I. S. (Bis, "मानक," *Bureau of Indian Standards*, vol. 875, no. 2, pp. 1–13, 1988.

[34] M. Kisan and S. Sangathan, "Iscus 383 (1970): Specification for coarse and fine aggregates from natural sources for concrete," vol. 2, 1970.

[35] B. of Indian Standards, "Is 1727 (1967): Methods of test for pozzolanic materials," 1968.

[36] Y. Zhao, J. Gao, C. Liu, X. Chen, and Z. Xu, "The particle-size effect of waste clay brick powder on its pozzolanic activity and properties of blended cement," *Journal of Cleaner Production*, vol. 242, Article ID 118521, 2020.

[37] K. G. Tsakalakis and K. G. Tsakalakis, "Conventional clinker grinding -A new approch to the prediction of power

consumption," 2020, http://www.min-eng.com/ultrafinegrinding06/paps.htmlhttp://www.min-eng.com/ultrafinegrinding06/paps.html.

[38] S. Wang, L. Baxter, and F. Fonseca, "Biomass fly ash in concrete: SEM, EDX and ESEM analysis," *Fuel*, vol. 87, no. 3, pp. 372–379, 2008.

[39] C. Rößler, B. Möser, and H.-M. Ludwig, "Characterization of cement microstructure by calculation of phase distribution maps from SEM-EDX mappings - pdf," in *Proceedings of the 19th Ibausil Conference*, Weimar/Germany, September 2015.

[40] S. J. Barnett, D. E. Macphee, E. E. Lachowski, and N. J. Crammond, "XRD, EDX and IR analysis of solid solutions between thaumasite and ettringite," *Cement and Concrete Research*, vol. 32.

[41] B. v. Bahoria, D. K. Parbat, and P. B. Nagarnaik, "XRD Analysis of Natural sand, Quarry dust, waste plastic (ldpe) to be used as a fine aggregate in concrete," *Materials Today Proceedings*, vol. 5, no. 1, pp. 1432–1438, 2018.

[42] "Particle size estimation and distributions," in *Mineral Processing Design and Operations*, pp. 33–69, Elsevier, Amsterdam, Netherlands, 2016.

[43] V. D. Katare and M. v. Madurwar, "Pozzolanic performance resemblance of milled sugarcane biomass ash using different pozzolanicity test methods," *Advances in Cement Research*, vol. 32, pp. 1–11, 2018.

[44] G. C. Cordeiro, R. D. Toledo Filho, L. M. Tavares, and E. M. R. R. Fairbairn, "Pozzolanic activity and filler effect of sugar cane bagasse ash in Portland cement and lime mortars," *Cement and Concrete Composites*, vol. 30, no. 5, pp. 410–418, May 2008.

[45] Brazilian Association of Technical Standards, *Pozzolans - Pozzolanic Activity - Determination of Pozzolanic Activity index with Portland Cement*, Vol. 5752, ABNT NBR, , Rio de Janeiro, Brazil, 1992.

[46] A.-N. 5752, *Determinação da atividadepozolâni- ca com cimento Portland. – Índice de atividadepozolânica com o cimento*, p. 5, AssociaçãoBrasileira de NormasTécnicas, Rio de Janeiro, 1992.

[47] A. Bahurudeen, M. S. Hemalatha, and M. Santhanam, *Need of an Efficient Procedure for the Evaluation of Pozzolanic Performance of Supplementary Cementitious Materials*, 2016.

[48] M. Frías and E. Villar-Cociña, "Influence of calcining temperature on the activation of sugar-cane bagasse: kinetic parameters," *Advances in Cement Research*, vol. 19, no. 3, pp. 109–115, July. 2007.

[49] M. P. Luxan, F. Madruga, and J. Saavedra, "Rapid evaluation of pozzolanic activity of natural products," *Cement and Concrete Research*, vol. 19, pp. 63–68, 1989.

[50] T. Ch Madhavi and S. Annamalai, "Electrical conductivity of concrete," vol. 11, no. 9, 2016, http://www.arpnjournals.com.

[51] G. P. Gava and L. R. Prudencio, "Pozzolanic activity tests as a measure of pozzolans' performance Part 1," *Magazine of Concrete Research*, vol. 59, no. 10, pp. 729–734, December. 2007.

[52] N. S. Ismael and M. N. Ghanim, "Properties of blended cement using metakaolin and hydrated lime," *Advances in Cement Research*, vol. 27, no. 6, pp. 321–328, December. 2015.

[53] G. C. Cordeiro, R. D. Toledo Filho, L. M. Tavares et al., "Experimental characterization of binary and ternary blended-cement concretes containing ultrafine residual rice husk and sugar cane bagasse ashes," *Construction and Building Materials*, vol. 29, pp. 641–646, April. 2012.

[54] Ibm and Indian Bureau of Mines (Ibm), *No Title Manual of procedure for chemical and instrumental analysis of ores, minerals, ore dressing products and environmental samples*, Indian Bureau of mines, Nagpur, 2012.

[55] V. D. Katare and M. V. Madurwar, "Design and investigation of sustainable pozzolanic material," *Journal of Cleaner Production*, vol. 242, Article ID 118431, 2020.

[56] E. Villar-Cociña, M. F. Rojas, E. V. Morales, and H. Savastano, "Study of the pozzolanic reaction kinetics in sugar cane bagasse-clay ash/calcium hydroxide system: kinetic parameters and pozzolanic activity," *Advances in Cement Research*, vol. 21, no. 1, pp. 23–30, Jan. 2009.

[57] M. Raverdy, "No Title Appreciation de l'activitepouzzolanique de constitutes secondaires," in *Proceedings of the 7e Congres International de la Chimie des Ciments*, Paris, France, 1980.

[58] A. T. Indore and M. Pradesh, "LIGHT HOUSE PROJECT INDORE 16034347690BuildingSanctionPlan.pdf,"pp. 1–22.

[59] M. Kisan and S. Sangathan, "Science progress," *Handbook on Functional Requirements of Buildings (Other than Industrial Buildings) [CED 12: Functional Requirements in Buildings]*, Vol. 41, Bureau of Indian Standards, New Delhi, 1987.

[60] S. S. Sinoh, Z. Ibrahim, F. Othman, L. M. Kuang, and A. Zaki, "Life cycle assessment of sugarcane bagasse ash as partial cement replacement in concrete," in *Proceedings of the e 4th International Conference on Sustainable Innovation 2020 –Technology, Engineering and Agriculture (ICoSITEA 2020)*, vol. 199, no. ICoSITEA 2020, pp. 144–150, Yogyakarta, Indonesia, October 2020.

[61] ASTM C311 - 07, "Standard test methods for sampling and testing fly ash or natural pozzolans for use in portland-cement concrete," vol. 1.

[62] M. V. Shoubi, "Reducing the operational energy demand in buildings using building information modeling tools and sustainability approaches," *Ain Shams Engineering Journal*, vol. 6, 2014.

[63] H. R. Gavali and R. v. Ralegaonkar, "Use of information modelling for urban poor housing," *SSRN Electronic Journal*, 2018.

[64] L. Lung, "Using BIM to simulate the energy consumption and reduce its cost," *International Journal of Innovation, Management and Technology*, vol. 10, no. 1, pp. 21–26, 2019.

[65] U. 662, "Indian standard method OF test for thermal conductivity OF thermal insulation materials BY means OF heat flow meter," 2008.

[66] C. Thormark, "The effect of material choice on the total energy need and recycling potential of a building," *Building and Environment*, vol. 41, no. 8, pp. 1019–1026, 2006.